The Canadian Mineralogist
Vol. 35, pp. 1283-1292 (1997)

STRUCTURE DETERMINATION OF VISTEPITE $SnMn_4B_2Si_4O_{16}(OH)_2$: ISOTYPISM WITH BUSTAMITE, REVISED CRYSTALLOGRAPHIC DATA AND COMPOSITION

JIŘÍ HYBLER[1], VÁCLAV PETŘÍČEK[1] AND KAREL JUREK[1]

Institute of Physics, Academy of Sciences of the Czech Republic, Cukrovarnická 10, 162 53 Praha 6, Czech Republic

ROMAN SKÁLA

Geological Survey, Geologická 6, 152 00 Praha 5, Czech Republic

IVANA CÍSAŘOVÁ

Department of Inorganic Chemistry, Faculty of Science of the Charles University, Hlavova 2030, 128 43 Praha 2, Czech Republic

Abstract

Vistepite, ideal composition $SnMn_4B_2Si_4O_{16}(OH)_2$, triclinic, $P\bar{1}$, *a* 6.973(2), *b* 7.365(2), *c* 7.665(1) Å, α 89.94(2), β 62.94(2), γ 76.88(2)°, *V* 339.05(10) Å^3, *Z* = 1, occurs in the rhodonite ore deposit on the northern flank of the Inyl'chek mountain chain, Tien-Shan, in southeastern Kirghizia. It forms tiny pale orange-yellow acicular crystals. A new electron-microprobe analysis yielded (in wt.%): Sn 13.70, Mn 27.91, Ca 0.71, Fe 0.28, Si 15.21, B 2.50, Al 0.27, O 36.64. The crystals are twinned, with [100] as twin axis and (010) as composition plane. The monoclinic unit-cell originally described by Pautov *et al.* (1992) corresponds to the *F*-centered cell of the twin lattice. In the structure analysis of cotype material, we used special procedures for the refinement of the structure involving twins. The refinement converged to $R = 4.15\%$ for 1244 observed reflections of both twin individuals ($R = 3.34\%$ for 968 observed reflections of one individual). One Sn and two independent Mn atoms are octahedrally coordinated. One B and two Si atoms occupy tetrahedrally coordinated positions. Corner-sharing tetrahedra form a *dreier* chain parallel to [100]. Edge-sharing octahedra form partially unoccupied infinite band, three octahedra wide, elongate along [100], with the plane of octahedra parallel to (011). Mn atoms occupy peripheral octahedra, whereas Sn atoms and vacancies alternate in central octahedra. This arrangement can be derived from the structure of bustamite if the Si(3) atom is replaced by B(1), and if the *M*1, *M*2, *M*3 octahedral positions are occupied by Mn(2), Mn(1), Sn(1) atoms, respectively, the *M*4 remaining vacant. The Sn(1) octahedron is smaller, and the vacant octahedron larger, than the corresponding octahedra of bustamite. Therefore, the adjacent Mn octahedra are deformed. A bond-valence calculation reveals that one oxygen atom, O(9), represents an OH group to maintain charge balance. The hydrogen atom has been found on the difference-Fourier map. The refinement revealed that the octahedrally coordinated position of Sn(1) is either partially vacant or partially substituted by Mn. Since several various triclinic unit-cells of bustamite have appeared in the literature, transformation matrices are provided. On the basis of results of the revision of cotype material for vistepite, we suggest a redefinition of the mineral species. The five most intense powder-diffraction maxima [*d* in Å(I)(*hkl*)] are: 3.392(100)(112, 201), 3.210(82)(01$\bar{2}$), 2.230(69)(01$\bar{3}$), 2.826(59)(2$\bar{1}$1) and 1.6952(56)(224, 004).

Keywords: vistepite, crystal structure, powder data, chain borosilicate, borosilicate of Sn and Mn, *dreier* chain of tetrahedra, twinning, redefinition of mineral species, Kirghizia.

Sommaire

La vistépite, de composition idéale $SnMn_4B_2Si_4O_{16}(OH)_2$ est triclinique, $P\bar{1}$, *a* 6.973(2), *b* 7.365(2), *c* 7.665(1) Å, α 89.94(2), β 62.94(2), γ 76.88(2)°, *V* 339.05(10) Å^3, *Z* = 1. On la trouve dans le gisement de rhodonite au flanc nord de la chaîne de montagnes Inyl'chek, Tien-Shan, dans le sud-est de la Kirghizie. Elle se présente en petits cristaux aciculaires, translucides et orange-jaune pâle. Une nouvelle analyse à la microsonde electronique a donné 13.70% Sn (en poids), 27.91% Mn, 0.71% Ca, 0.28% Fe, 15.21% Si, 2.50% B, 0.27% Al, 36.64% O. Les cristaux sont maclés selon l'axe [100], avec (010) comme plan de composition. La maille proposée par Pautov *et al.* (1992) correspond à la maille *F*-centrée du réseau de la macle. L'analyse de sa structure a été faite en utilisant les procédures spécialisées pour l'affinement des macles. L'indice $R = 4.15\%$ a été atteint en utilisant 1244 réflexions observées pour les deux individus de la macle ($R = 3.34$ % pour 968 réflections observées sur un individu). Le Sn occupe une position indépendante, et le Mn, deux; ces atomes sont en coordinence octaédrique. Un atome de B et deux atomes de Si sont en coordinence tetraédrique. Les tetraèdres s'articulent par partage de

[1] *E-mail addresses*: hybler@fzu.cz, petricek@fzu.cz, jurek@fzu.cz, skala@cgu.cz, cisarova@prfdec.natur.cuni.cz

coins en chaînes *dreier* infinies parallèles à [100]. Les octaèdres à arêtes partagées se présentent en bandes à trois rangées parallèles avec [100], le plan des octaèdres étant parallèle avec (011). Les octaèdres des rangées latérales sont tous occupés par Mn, tandis que dans la rangée centrale alternent un atome de Sn et une lacune. On peut dériver cette structure de celle de la bustamite en remplaçant la position Si(3) par B(1), en plaçant Mn(2), Mn(1) et Sn(1) sur les positions *M*1, *M*2, *M*3, respectivement, et en laissant la position *M*4 vide. En comparaison de ces structures, le tetraèdre B(1) est plus petit que le tetraèdre Si(3), l'octaèdre Sn(1) est aussi plus petit que *M*3, l'octaèdre vide est plus gros que *M*4, et les octaèdres à Mn sont plus difformes que ceux de la bustamite. Le calcul des valences des liaisons a identifié un atome d'oxygène, O(9), comme groupe OH, ce qui est nécessaire pour maintenir la balance des charges. On a localisé l'atome d'hydrogène sur la projection de différence Fourier. L'octaèdre Sn(1) est en partie vacant ou remplacé par Mn. Plusieurs mailles tricliniques centrées de la bustamite étant citées dans la littérature, nous présentons les matrices de transformation entre ces mailles et celle de la vistépite. Nous redéfinissons la vistépite à la lumière des résultats obtenus sur matériau cotype. Les cinq raies les plus intenses du cliché de diffraction obtenu par la méthode des poudres [*d* en Å(I)(*hkl*)] sont: 3.392(100)(112, 201), 3.210(82)(01$\bar{2}$), 2.230(69)(01$\bar{3}$), 2.826(59)($2\bar{1}1$) et 1.6952(56)(224, 004).

Mots-clés: vistépite, structure cristalline, diffraction X (méthode des poudres), borosilicate à chaînes, borosilicate de Sn et Mn, chaîne des tetraèdres *dreier*, macle, redéfinition d'espèce minérale, Kirghizie.

INTRODUCTION

Vistepite was found in the rhodonite deposit on the northern flank of the Inyl'chek mountain chain in southeastern Kirghizia in 1987. Pautov *et al.* (1992) described the occurrence and its paragenesis. Vistepite is translucent, pale orange-yellowish in color and with a vitreous luster. A chemical analysis using electron microprobe, laser spectral micro-analysis and determination of boron by colorimetric titration, all done by these authors, gave as the empirical formula: $(Mn_{4.84}Ca_{0.10}Fe_{0.05})_{\Sigma 4.99}Sn_{1.02}B_{2.00}(Si_{4.90}Al_{0.11})_{\Sigma 5.01}O_{20}$. The corresponding ideal formula is $Mn_5SnB_2Si_5O_{20}$. They reported a monoclinic cell with *a* 28.77(1), *b* 7.01(2), *c* 13.72(2) Å, β 96.6(2)°, *V* 2749(9) Å^3, space group *P2/m*.

Our investigation of the crystal structure of this species was made on cotype material from the original locality. This material is deposited in the National Museum, Prague, Czech Republic under numbers P1N 84596 (single crystals) and P1N 82890 (polished section).

REVISED CHEMICAL COMPOSITION

A polished section of a tiny fragment (~0.4 mm) of vistepite was analyzed with the JEOL Superprobe 733 electron-probe micro-analyzer. The operating voltage was 15 kV, and the sample current, ~30 nA. For detection of light elements (B, O), a wavelength-dispersion spectrometer with the nickel–carbon multilayer (2*d* = 84 Å) was employed, whereas the ordinary spectrometers were used for the other elements. The following standards were used: quartz (Si, O), hematite (Fe), corundum (Al), diopside (Ca), pure metals (Sn, Mn) and borosilicate glass (B) of known boron content (4.866 wt.%, determined by wet-chemical analysis). Sn*L*α and *K*α lines of other elements were used for analysis. The data were corrected by the program STRATA (Pichoir & Pouchou 1991). Average results of 10 point analyses are shown in Table 1. Because of some problems with boron and oxygen detection, the total sum is somewhat below 100%.

Since the results of the structure analysis (see later) revealed 16 atoms of oxygen plus two OH groups per formula unit, the revised formula, normalized on 18 atoms of oxygen should be written: $(Mn_{3.99}Ca_{0.13}Fe_{0.04})_{\Sigma 4.16}Sn_{0.91}B_{1.81}(Si_{4.25}Al_{0.08})_{\Sigma 4.33}O_{16}(OH)_2$.

TABLE 1. REVISED CHEMICAL COMPOSITION OF VISTEPITE

element	average (in wt.%)	e. s. d.	min. value	max. value	atomic %
Sn	13.70	0.49	13.10	14.70	2.91
Mn	27.91	0.21	27.60	28.30	12.78
Ca	0.71	0.20	0.46	0.98	0.42
Fe	0.28	0.08	0.14	0.36	0.13
Si	15.21	0.25	15.00	15.80	13.62
B	2.50	0.12	2.30	2.70	5.80
Al	0.27	0.06	0.18	0.42	0.26
O	36.64	1.14	35.80	39.80	57.67
H*	0.25				6.41
Total:	97.47				

* Calculated value. The results represent an average of ten point-analyses obtained with an electron microprobe.

SINGLE-CRYSTAL X-RAY INVESTIGATION

A re-investigation of the original precession photographs showed that the unit cell referred to by Pautov *et al.* (1992) is not primitive, but *F*-centered, ($h + k = 2n$, $k + l = 2n$, $h + l = 2n$). A new *C*-centered unit cell has been proposed here with *a* 13.72, *b* 7.01, *c* 15.21 Å, β 110.0 °, *V* 1348 Å^3.

Weissenberg photographs of the *h*0*l*, *h*1*l*, *h*2*l*, *h*3*l* reciprocal lattice planes revealed unusual extinction conditions ($h = 4n$ for *h*00, $k = 4n$ for *k*00), as well as splitting of diffraction spots on even layers (with exception of the zero layer), whereas diffraction spots on odd layers are unsplit. This splitting seems to be due to the imperfect overlay of diffraction spots of twin individuals with (reduced) cell parameters *a* 6.973, *b* 7.365, *c* 7.665 Å, α 89.94, β 62.94, γ 76.88°,

V 339.02 Å^3. The above-mentioned centered cells represent, therefore, a twin lattice.

The transformation matrices of the lattice vectors from the cell of Pautov *et al.* (1992) are (0, ¼, 0 / –1, – ¼, – ½ / 0, 0, ½) and (0, – ¼, 0 / –1, – ¼, – ½ / 0, 0, – ½) for the first and the second twin individual, respectively. The twin operation is a two-fold axis parallel to the [100] vector of the reduced cell, represented by the twin matrix (1, ½, 1 / 0, –1, 0 / 0, 0, –1). All matrices [P] used in this paper obey the formula [**a'**, **b'**, **c'**] = [**a**, **b**, **c**] x [P], as introduced by Arnold (1983, 1989).

TABLE 2. MISCELLANEOUS INFORMATION CONCERNING VISTEPITE

a [Å]	6.973(2)	Crystal size [mm]	0.032 × 0.045 × 0.210
b	7.365(2)	radiation	MoK_α / Graphite
c	7.665(1)	No. of intensities	1784
α [°]	89.94(2)	No. of $I_o > 3\sigma(I_o)$	1244
β	62.94(2)	min. transmission	0.529
γ	76.88(2)	max. transmission	0.798
V [Å^3]	339.05(10)	R(obs.) %	4.15
Sp. Gr.	$P\bar{1}$	wR(obs.) %	4.48
Z	1	S	2.03
μ [mm^{-1}]	5.766		
D_o [g.cm^{-3}]	3.72		

Cell content : 1[$SnMn_4Si_4B_2O_{16}(OH)_2$]

$R = \Sigma(|F_o| - |F_c|) / \Sigma|F_o|$

$wR = [\Sigma w(|F_o| - |F_c|)^2 / \Sigma F_o^2]^{1/2}$, $w = 1 / (\sigma^2(F_o) + (0.01\,|F_o|)^2)$

Experimental

Two sets of diffraction data were collected, one on an Enraf–Nonius CAD4 diffractometer and the other on a Hilger & Watts diffractometer. Experimental details are listed in Table 2. The intensities were corrected for the Lorentz and polarization factors and absorption according to the crystal shape (AGNOST C, Templeton & Templeton 1978, adapted by M. Dušek, pers. commun.). All calculations were done using the package of programs SDS (Petříček & Malý 1990, Petříček 1994).

Structure Solution and Refinement

The structure has been solved by the Patterson method. The correct positions of heavy atoms were found using the Patterson map constructed from unsplit reflections of one twin individual; the remaining atoms were found on the Fourier map. The full-matrix refinement included reflections of both individuals, using a special procedure for refinement of twins. Scattering factors were taken from *International Tables for X-ray Crystallography* (1974). The final R is 4.15% for 1244 observed reflections of both twin individuals (R = 3.34% for 968 observed reflections of one individual).

There are one Sn, two Mn and Si, one B and nine oxygen atoms in independent atomic positions. Atomic coordinates and anisotropic thermal parameters are listed in Table 3, selected interatomic distances in Table 4, and bond valences in Table 5. Observed and calculated structure-factors have been deposited with the Depository of Unpublished Data, CISTI, National Research Council of Canada, Ottawa, Ontario K1A 0S2.

The refinement showed a partial lack of diffracting mass in the position of the Sn atom, which could be

TABLE 3. FRACTIONAL COORDINATES AND DISPLACEMENT FACTORS (×10^2) FOR VISTEPITE

Atom	site	x	y	z	U_{11}	U_{22}	U_{33}	U_{12}	U_{13}	U_{23}	U_{eq}
Sn(1)	1*a*	0	0	0	0.67(5)	0.90(5)	0.44(5)	-0.21(4)	-0.09(4)	0.16(3)	0.73(4)
Mn(1)	2*i*	0.8108(3)	0.2762(2)	-0.2634(2)	1.29(8)	1.65(7)	0.76(7)	-0.41(7)	-0.28(7)	0.28(5)	1.31(6)
Mn(2)	2*i*	0.3042(2)	0.2866(2)	-0.2623(2)	0.83(8)	1.56(7)	0.95(7)	-0.11(6)	-0.07(7)	0.26(5)	1.23(6)
Si(1)	2*i*	0.0742(4)	0.3274(3)	0.2426(3)	0.6(1)	1.3(1)	0.7(1)	-0.36(9)	-0.2(1)	0.30(9)	0.9(1)
Si(2)	2*i*	0.5327(4)	0.3252(3)	0.2216(3)	0.6(1)	1.5(1)	0.6(1)	-0.3(1)	-0.1(1)	0.22(9)	1.0(1)
B(1)	2*i*	-0.252(2)	0.122(1)	0.431(1)	1.2(5)	1.3(4)	0.7(4)	-0.7(4)	-0.5(4)	0.5(4)	1.0(4)
O(1)	2*i*	-0.141(1)	-0.0431(7)	0.2885(8)	1.5(3)	1.3(3)	1.2(3)	-0.7(3)	-0.5(3)	0.3(2)	1.3(3)
O(2)	2*i*	0.1201(9)	0.2174(8)	0.0375(8)	1.7(3)	1.7(3)	0.9(3)	-0.9(3)	-0.5(3)	0.2(2)	1.4(3)
O(3)	2*i*	0.5650(9)	0.2549(8)	0.4109(8)	1.2(3)	1.7(3)	1.2(3)	-0.1(3)	-0.6(3)	-0.1(3)	1.4(3)
O(4)	2*i*	0.7282(9)	0.1939(7)	0.0237(8)	1.3(3)	1.4(3)	1.2(3)	-0.4(2)	-0.6(3)	0.5(2)	1.3(3)
O(5)	2*i*	-0.0897(9)	0.2296(8)	0.4247(9)	1.0(3)	1.5(3)	1.1(3)	-0.9(2)	-0.4(3)	0.3(3)	1.2(2)
O(6)	2*i*	0.3012(9)	0.2750(8)	0.2618(8)	1.3(3)	2.0(3)	1.5(3)	-0.9(3)	-0.4(3)	0.7(2)	1.6(3)
O(7)	2*i*	-0.016(1)	0.5495(7)	0.2636(8)	1.4(3)	1.3(3)	1.7(3)	-0.2(3)	-0.8(3)	0.1(2)	1.5(3)
O(8)	2*i*	0.513(1)	0.5445(7)	0.2045(8)	1.3(3)	1.6(3)	1.4(3)	-0.4(3)	-0.6(3)	0.1(2)	1.5(3)
O(9)	2*i*	-0.357(1)	0.0827(8)	0.6397(8)	1.2(3)	1.6(3)	0.7(3)	-0.6(3)	-0.1(3)	0.5(2)	1.2(2)
H(1)	2*i*	0.32(3)	0.02(2)	0.33(2)							10.0*)

*) Fixed value

TABLE 4. SELECTED INTERATOMIC DISTANCES [Å] IN VISTEPITE

Sn(1) octahedron		Mn(1) octahedron		Mn(2) octahedron	
Sn(1) - O(1)	2.030(6) × 2	Mn(1)- O(1)	2.467(7)	Mn(2)- O(1)	2.385(7)
Sn(1) - O(2)	2.044(7) × 2	Mn(1)- O(4)	2.131(6)	Mn(2)- O(2)	2.191(6)
Sn(1) - O(4)	2.030(6) × 2	Mn(1)- O(5)	2.167(7)	Mn(2)- O(3)	2.302(5)
Mean	2.035(6)	Mn(1)- O(7)	2.126(8)	Mn(2)- O(7)	2.101(7)
		Mn(1)- O(8)	2.183(7)	Mn(2)- O(8)	2.145(8)
		Mn(1)- O(9)	2.349(8)	Mn(2)- O(9)	2.272(6)
		Mean	2.237(7)	Mean	2.233(7)
Si(1) tetrahedron		Si(2) tetrahedron		B(1) tetrahedron	
Si(1) - O(2)	1.630(7)	Si(2) - O(3)	1.633(8)	B(1) - O(1)	1.44(1)
Si(1) - O(5)	1.641(6)	Si(2) - O(4)	1.618(5)	B(1) - O(3)	1.49(1)
Si(1) - O(6)	1.615(8)	Si(2) - O(6)	1.630(8)	B(1) - O(5)	1.50(1)
Si(1) - O(7)	1.593(6)	Si(2) - O(8)	1.600(6)	B(1) - O(9)	1.49(1)
Mean	1.619(7)	Mean	1.620(7)	Mean	1.48(1)
O(9) - H(1)	0.8(1)				
O(6) - H(1)	2.0(1)				
B(1) - H(1)	2.0(2)				

explained either by a partial occupancy [with probability 0.897(3)] of this position, or by a partial replacement of Sn by Mn in the ratio 0.792(3):0.208. Both possibilities were considered and modeled, but there were no substantial differences in the *R*-value. This problem is discussed later.

Since the chemical analysis revealed small amounts of Ca, Fe and Al, the partial replacement of some atoms was therefore taken into the account. The refinement gave possible substitution of Ca for Mn in the Mn(1) position in the ratio 0.07:0.93(3), whereas the Mn(2) position is fully occupied by Mn. The substitution Fe for Mn and Al for Si could not be refined because of the small difference between the atomic scattering factors.

TABLE 5. VISTEPITE: BOND-VALENCE TABLE

Atom	Sn(1)	Mn(1)	Mn(2)	Si(1)	Si(2)	B(1)	Σ
O(1)	$0.71^{\times 2}\downarrow$	0.16	0.20	-	-	0.82	**1.89**
O(2)	$0.68^{\times 2}\downarrow$	-	0.33	1.02	-	-	**2.03**
O(3)	-	-	0.25	-	0.95	0.72	**1.92**
O(4)	$0.71^{\times 2}\downarrow$	0.41	-	-	0.98	-	**2.10**
O(5)	-	0.35	-	0.95	-	0.73	**2.03**
O(6)	-	-	-	1.00	1.04	-	**2.04**
O(7)	-	0.40	0.43	1.05	-	-	**1.88**
O(8)	-	0.34	0.38	-	1.10	-	**1.82**
O(9)	-	0.22	0.27	-	-	0.72	**1.21**
Σ	**4.20**	**1.88**	**1.86**	**4.02**	**4.07**	**2.99**	

The parameters were taken from Brese & O'Keeffe (1991).

The electron-microprobe analysis revealed also a relative surplus of Si and a deficiency of B. An attempt to replace a certain part of B in the B(1) position by Si was rejected in the refinement procedure.

The bond-valence table identified one atom of oxygen O(9), as part of an OH group (Table 5). We attempted to find a hydrogen atom on the difference Fourier map. In addition to false peaks close to heavy atoms, one peak at a reasonable distance (0.8 Å) from O(9), at $x \approx 0.42$, $y \approx 0$, $z \approx 0.29$ was found. The refined position of this atom, denoted as H(1), is shown in Table 3, and its distances from O(9) and O(6) are listed in Table 4.

Description of the Structure and Discussion

Sn and Mn atoms are octahedrally coordinated [positions Sn(1), Mn(1), Mn(2)], whereas the Si and B atoms are tetrahedrally coordinated [(positions Si(1), Si(2) and B(1)]. There are eight oxygen atoms, and, as indicated by bond-valence calculation, one (OH) group. Therefore, the ideal formula of vistepite, based on results of the structure analysis, and neglecting minor elements and a partial shortage in the amount of tin, should be written as $SnMn_4B_2Si_4O_{16}(OH)_2$ (instead of $SnMn_5B_2Si_5O_{20}$). This result is in an acceptable agreement with the revised results of the electron-microprobe analyses, with the exception of the boron and silicon content.

The main structural features are as follows (Fig. 1): (1) infinite chains of tetrahedra, parallel to **a**, unbranched, with repetition period three (*dreier* chains of Liebau 1985), with two Si tetrahedra and one B tetrahedron, and the repetition sequence [–Si(1)–Si(2)–B(1)–]$_\infty$; (2) bands of edge-sharing octahedra, three octahedra wide, with the plane of octahedra parallel to (011) and oriented along **a**. On Figure 2, these chains and bands are seen perpendicular to their length. The peripheral octahedra are occupied by Mn atoms [Mn(1) and Mn(2)], whereas in the central positions, Sn atoms alternate with vacancies. The Sn(1) octahedron is small (average Sn–O = 2.034 Å) and almost regular, whereas the vacant octahedron is larger (average □ – O = 2.559 Å). Both Mn(1) and Mn(2) octahedra are deformed and somewhat larger than the Sn(1) octahedron. The B(1) tetrahedron is somewhat smaller than the Si(1) and Si(2) tetrahedra (Table 4, Fig. 1).

Each band of octahedra is linked to other bands *via* six *dreier* chains, and each chain is attached to three bands of octahedra.

Similar *dreier* chains and bands of octahedra of the same width are present in the structures of wollastonite $CaSiO_3$, bustamite $(Ca,Mn)SiO_3$, and ferrobustamite $(Ca,Fe)SiO_3$ (Peacor & Buerger 1962, Peacor & Prewitt 1963, Prewitt & Peacor 1964, Rappoport & Burnham 1973, Ohashi & Finger 1976, 1978, Yamanaka *et al.* 1977). In these structures, all tetrahedra are occupied by Si, and octahedral sites are fully occupied by Ca and Mn or Fe atoms. The structure of vistepite is related to that of bustamite (Fig. 3a) as follows: B(1) substitutes for silicon in the Si(3) tetrahedron, positions Mn(2) and Mn(1) correspond to the *M*1 and *M*2 positions in bustamite, Sn(1) corresponds to *M*3, and the vacancy, to *M*4 in bustamite. These octahedra are placed at the centers of inversion. In the wollastonite structure (Fig. 3b), there is only one central octahedron position *M*3, and inversion centers are on shared edges of these octahedra. This is because all octahedra are fully occupied by Ca. The composition of bustamite (and of ferrobustamite) varies widely, and the occupancies and sizes of the octahedra depend on the Ca:Mn (or Ca:Fe) ratio (Ohashi & Finger 1978). In the central octahedron,

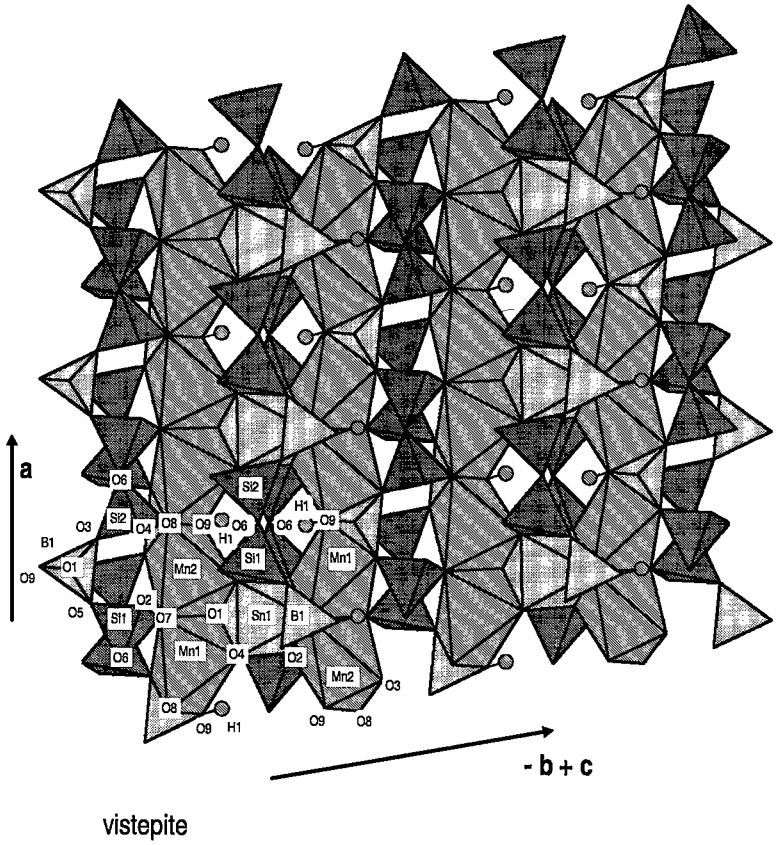

FIG. 1. The structure of vistepite, projected onto (011). Bands of octahedra oriented along **a** are stacked parallel to this plane and linked to each other by *dreier* chains of tetrahedra. Hydrogen atoms are indicated as small circles.

Mn enters preferentially the *M*3, and Ca, the *M*4 site. Therefore, the *M*4 octahedron is somewhat larger (mean *M*4 – O ≈ 2.37–2.43 Å) than *M*3 (mean *M*3 – O ≈ 2.18–2.19 Å). In vistepite, the central octahedra differ more in size and occupancy, the Sn(1) octahedron being smaller and the vacant octahedron larger than the *M*3 and *M*4 octahedra in bustamite (Table 4). Vistepite also differs from bustamite by the presence of one OH group [O(9)] to maintain charge balance, as discussed above.

Another question to be discussed is the shortage of diffracting mass in the Sn position. The refined occupancy-factor is 0.897, and the supposed partial replacement of Sn by Mn gave the ratio 0.792:0.208. The formula based on results of the electron-microprobe analyses seems to favor the first possibility, but there is also a very small amount of Ca and Fe replacing Mn. Therefore, Mn or Fe could, at least partially, enter the Sn(1) position. Charge balance could be achieved by a partial replacement of Mn^{2+} by Mn^{3+}, Fe^{3+} or Mn^{4+}. The presence of these cations could be determined by spectroscopic methods, but unfortunately there is not enough material available for this study.

The remaining discrepancy in the Si:B ratio could perhaps be explained by a possible variability in the composition of vistepite, as it is known in the case of bustamite. However, the collected electron-microprobe data have revealed only small inhomogeneities within one single grain available for this study. This possibility can be evaluated only with more extensive analytical studies, for which a larger number of vistepite grains would be necessary.

Vistepite, bustamite and ferrobustamite are triclinic. Most authors use centered triclinic cells, which can be more convenient, as they have some angles close to 90°. Besides the reduced cell used in this paper, the following cells are used: *P* (primitive) by Berman & Gonyer (1937), here referred to as the *BG* cell (probably

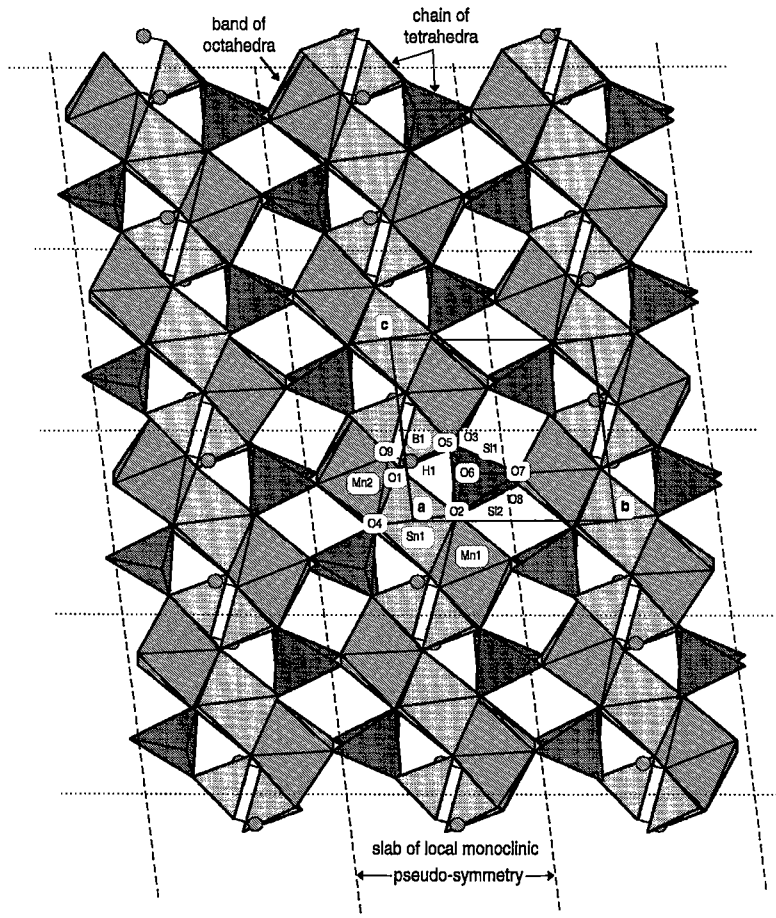

FIG. 2. The structure of vistepite projected approximately down **a** of the reduced cell. *Dreier* chains of tetrahedra and bands of octahedra are almost perpendicular to the plane of projection. The unit cell is indicated by full lines, and the boundaries of slabs of local monoclinic pseudosymmetry (OD-layers) are marked by broken lines. Subunits within slabs, which are mutually shifted by **a**/2, are indicated by dotted lines.

wrongly derived by use of an analogy with wollastonite), *F*-centered of Peacor & Buerger (1962), *i.e.*, *PB* cell, *A*-centered of Peacor & Prewitt (1963), (the *PP* cell), and *I*-centered of Ohashi & Finger (1976, 1978) (the *OF* cell). This last cell has **c** parallel to the chain of tetrahedra, and (100) parallel to the plane of bands of octahedra. Corresponding unit-cell parameters of bustamite are listed in Table 6. In Table 7, matrices for transformation of cell parameters among all these cells are given.

TWINNING

The mechanism of twinning is the same as that for bustamite and ferrobustamite, and very similar to that for wollastonite and pectolite (Prewitt & Buerger 1963, Peacor & Prewitt 1963, Prewitt & Peacor 1964). It can be described as follows. The band of octahedra has a monoclinic pseudosymmetry. The pseudo-two-fold axis is parallel to **a**, and passes through the Sn atoms and vacancy centers. There are also pseudo-mirror planes

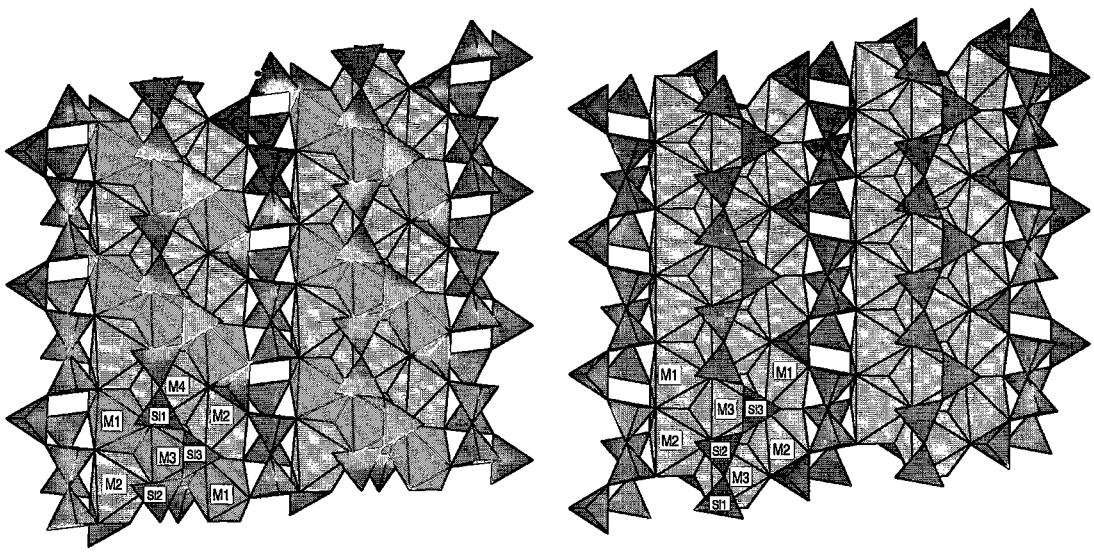

(a) bustamite (b) wollastonite

FIG. 3. The crystal structures of (a) bustamite and (b) wollastonite (according to Ohashi & Finger 1978) in the same orientation as the structure of vistepite in Figure 1.

TABLE 6. UNIT-CELL PARAMETERS OF BUSTAMITE AND FERROBUSTAMITE IN VARIOUS CHOICES OF UNIT CELL

cell	*OF* - cell	*PP* - cell	*PB* - cell	*BG* - cell
reference	Ohashi & Finger 1978	Peacor & Prewitt 1963	Peacor & Buerger 1962	Berman & Gonyer 1937
mineral	bustamite	bustamite	bustamite	bustamite
a[Å]	9.864(4)	7.736	15.412	7.64
b	10.790(5)	7.157	7.157	7.16
c	7.139(3)	13.824	13.824	6.87
α[°]	99.53(4)	90.52	89.48	92.13
β	99.71(3)	94.58	94.85	94.91
γ	83.83(5)	103.87	102.93	101.58
V[Å^3]	736.1(5)	740.4	1480.7	366.2
space group	$I\bar{1}$	$A\bar{1}$	$F\bar{1}$	$P\bar{1}$

The unit-cell edge length corresponding to the apparent two-fold (or twin) axis is underlined.

perpendicular to this pseudo-axis, with **a**/2 spacing, so that the atoms Sn(1), B(1), O(1), O(6), O(8) and O(9) are in pseudo-special positions on these planes. This pseudo-symmetry is maintained in four of six adjacent chains of tetrahedra. These chains connect the band of octahedra with adjacent bands *via* (001) and (00$\bar{1}$) planes. Adjacent bands are shifted vertically by (approximately) **a**/2 with respect to the reference plane perpendicular to [100], but otherwise the monoclinic pseudosymmetry 2/*m* is maintained for the slab parallel to (010) and is one unit cell thick. The position of this slab is indicated on Figure 2. This alternation of the position of the band of octahedra led some authors to use centered cells for bustamite. The bands of octahedra, parallel to (011), are stacked diagonally within this slab. The remaining two chains of tetrahedra connect this slab to adjacent slabs. The arrangement of shared O-atoms of these chains ensures that the adjacent slabs are shifted approximately by ±**a**/4 with respect to the starting slab. This shift breaks the local monoclinic pseudosymmetry because the local planes of pseudosymmetry have no continuity. Such a structure can be interpreted as an example of a desymmetrized OD-structure, where slabs with the local pseudosymmetry represent OD-layers, and their ±**a**/4 shifts the vicinity condition. For details about OD-structures, see for example Ďurovič (1992).

In one twin individual, consecutive slabs (OD-layers) are shifted in the same sense; this is reversed at the twin boundary. The compositional plane of the twin is therefore (010), identical with the plane of the slabs. In wollastonite (and also in pectolite, where *dreier* chains are combined with bands of octahedra two octahedra wide), the local monoclinic pseudosymmetry in slabs (OD-layers) is $2_1/m$ because of the different arrangement of bands of octahedra and chains of tetrahedra (Ohashi & Finger 1978). There is no alternation of positions of the bands of octahedra within the slab in these structures. Otherwise, the mechanism of twinning is the same.

The same mechanism is responsible for polytypism. The monoclinic polytype *2M* of wollastonite has regular alternation of shifts corresponding to +**a**/4 and −**a**/4 (Trojer 1968, Hesse 1984, Ohashi 1984). A similar *2M* polytype of bustamite was determined by Hesse *et al.* (1982). Some rare triclinic polytypes of wollastonite

TABLE 7. TRANSFORMATION MATRICES [*P*] FOR VARIOUS UNIT-CELLS OF BUSTAMITE, FERROBUSTAMITE AND VISTEPITE

to cell → / from cell ↓	*reduced triclinic cell, this work*	*OF- cell*	*PP - cell*	*PB - cell*	*BG - cell*
reduced triclinic cell, this work	----------	$\begin{bmatrix} 1 & 0 & -1 \\ -1 & -1 & 0 \\ -1 & 1 & 0 \end{bmatrix}$	$\begin{bmatrix} 0 & -1 & -1 \\ 1 & 0 & 0 \\ 0 & 0 & 2 \end{bmatrix}$	$\begin{bmatrix} 1 & -1 & 1 \\ -2 & 0 & 0 \\ 0 & 0 & -2 \end{bmatrix}$	$\begin{bmatrix} 1/2 & -1 & 1/2 \\ -1 & 0 & 0 \\ 0 & 0 & -1 \end{bmatrix}$
OF - cell	$\begin{bmatrix} 0 & -1/2 & -1/2 \\ 0 & -1/2 & 1/2 \\ -1 & -1/2 & -1/2 \end{bmatrix}$	----------	$\begin{bmatrix} -1/2 & 0 & -1 \\ -1/2 & 0 & 1 \\ -1/2 & 1 & 0 \end{bmatrix}$	$\begin{bmatrix} 1 & 0 & 1 \\ 1 & 0 & -1 \\ 0 & 1 & 0 \end{bmatrix}$	$\begin{bmatrix} 1/2 & 0 & 1/2 \\ 1/2 & 0 & -1/2 \\ 0 & 1 & 0 \end{bmatrix}$
PP - cell	$\begin{bmatrix} 0 & 1 & 0 \\ -1 & 0 & -1/2 \\ 0 & 0 & 1/2 \end{bmatrix}$	$\begin{bmatrix} -1 & -1 & 0 \\ -1/2 & -1/2 & 1 \\ -1/2 & 1/2 & 0 \end{bmatrix}$	----------	$\begin{bmatrix} -2 & 0 & 0 \\ -1 & 1 & 0 \\ 0 & 0 & -1 \end{bmatrix}$	$\begin{bmatrix} -1 & 0 & 0 \\ 1/2 & 1 & 0 \\ 0 & 0 & -1/2 \end{bmatrix}$
PB - cell	$\begin{bmatrix} 0 & -1/2 & 0 \\ -1 & -1/2 & -1/2 \\ 0 & 0 & -1/2 \end{bmatrix}$	$\begin{bmatrix} 1/2 & 1/2 & 0 \\ 0 & 0 & 1 \\ 1/2 & -1/2 & 0 \end{bmatrix}$	$\begin{bmatrix} -1/2 & 0 & 0 \\ -1/2 & 1 & 0 \\ 0 & 0 & -1 \end{bmatrix}$	----------	$\begin{bmatrix} 1/2 & 0 & 0 \\ 0 & 1 & 0 \\ 0 & 0 & 1/2 \end{bmatrix}$
BG - cell	$\begin{bmatrix} 0 & -1 & 0 \\ -1 & -1/2 & -1/2 \\ 0 & 0 & -1 \end{bmatrix}$	$\begin{bmatrix} 1 & 1 & 0 \\ 0 & 0 & 1 \\ 1 & -1 & 0 \end{bmatrix}$	$\begin{bmatrix} -1 & 0 & 0 \\ -1/2 & 1 & 0 \\ 0 & 0 & -2 \end{bmatrix}$	$\begin{bmatrix} 2 & 0 & 0 \\ 0 & 1 & 0 \\ 0 & 0 & 2 \end{bmatrix}$	----------

Transformation formula: [**a'**, **b'**, **c'**] = [**a**, **b**, **c**] × [*P*].

with various sequences were described by Henmi *et al.* (1978, 1983). Thus it can be expected that crystals of vistepite may be twinned, untwinned or polytypic, similar to the cases of wollastonite, bustamite, ferrobustamite and pectolite.

Revised Powder-Diffraction Data

Since the original description of vistepite contained only camera data of poor quality, new powder-diffraction data were also collected. Several small crystals were selected under a binocular lens, then crushed and coated from alcohol suspension on a flat glass sample holder. The powder pattern was collected using a HZG–4 goniometer in Bragg–Brentano θ–2θ reflecting geometry. A TuR M62 X-ray generator was operated at 30 kV and 40 mA. The measuring radius of goniometer was set to 250 mm, the Soller collimator 0.5/0.50 mm was placed between the X-ray tube and the sample. Cu*K*α radiation was filtered with a primary Ni-filter. Step-scanning with step width of 0.02° 2θ and an exposure of 17 seconds per step provided data, which were further evaluated by the version 6.01 of the program ZDS (Ondruš 1995). The Pearson VII profile shape function, which allows modeling of the asymmetrical $\alpha_1\alpha_2$ doublet, approximated positions of individual reflections. The powder pattern was indexed to match the theoretical powder pattern generated from the crystal structure, as refined from the measured single-crystal data, by the program LAZY PULVERIX (Yvon *et al.* 1977). Unit-cell parameters obtained from the powder data are fairly consistent with those from the single-crystal study. Observed and calculated *d*-values, *hkl* indices corresponding to the primitive triclinic cell, observed intensities and unit-cell parameters are summarized in Table 8.

Redefinition of the Species

Based on the results of the aforementioned revision of the cotype material for vistepite, we suggest to redefine vistepite as a triclinic species, with the space group $P\bar{1}$, and the ideal chemical formula $SnMn_4B_2Si_4O_{16}(OH)_2$. The proposal was approved by the CNMMN of the IMA.

Acknowledgements

The authors are grateful to Dr. L. A. Pautov from the Museum of Il'men Reserve, Miass, Russia, for supplying the specimens, to Drs. M. Dušek, L. Červinka and J. Fábry from the Institute of Physics, Czech Academy of Sciences for computational help. Dr. F. Veselovský from the Geological Survey, Prague, kindly prepared polished sections of vistepite and the borosilicate glass used as standard. We also thank Dr. J. Fábry for valuable discussion and Ing. Ctirad Novák and Dr. L. Jilemnická for critically reading the manuscript. The authors also express their gratitude to Associate Editor Dr. F.C. Hawthorne and to the referees for their comments. All illustrations were prepared using the program ATOMS (Dowty 1991). This study has been supported by grants No. 202/93/0085 and 203/96/0111 of the Grant Agency of the Czech Republic. Powder data were processed using the ZDS software purchased from the project of the Grant Agency of the Czech Republic No. 205/95/0980.

TABLE 8. REVISED X-RAY POWDER-DIFFRACTION DATA OF VISTEPITE (*d* IN Å)

I/I_0	d_{obs}	d_{calc}	*hkl*	I/I_0	d_{obs}	d_{calc}	*hkl*	I/I_0	d_{obs}	d_{calc}	*hkl*	I/I_0	d_{obs}	d_{calc}	*hkl*
3.5	7.15	7.12	010	58.8	2.826	2.824	2-11	1.8	2.0700	2.0626	03-2	11.4	1.6339	1.6351	2-33
20.1	6.79	6.78	001	35.4	2.801	2.796	221	6.7	2.0588	2.0521	2-20	7.6	1.6242	1.6243	24-1
8.3	6.15	6.13	101	4.8	2.674	2.673	2-12	7.3	2.0476	2.0449	303	8.6	1.5356	1.5336	404
9.1	6.01	6.01	100	3.1	2.655	2.653	220	6.8	2.0371	2.0326	232	8.0	1.5248	1.5306	420
10.2	5.314	5.306	110	19.5	2.613	2.615	02-2	14.1	1.8725	1.8751	104	3.5	1.5036	1.5034	2-3-1
9.5	5.068	5.042	111	13.1	2.544	2.541	103	0.1	1.8654	1.8648	331	7.3	1.4976	1.4992	2-15
24.2	4.658	4.640	011	11.6	2.510	2.512	11-2	3.0	1.8551	1.8585	20-2			1.4978	22-3
15.8	4.340	4.332	1-11	8.6	2.4925	2.4954	10-2			1.8519	214	0.3	1.4763	1.4765	315
9.9	4.115	4.104	1-10	8.6	2.4295	2.4301	203	4.5	1.8440	1.8431	032	10.8	1.4626	1.4652	2-34
6.7	3.808	3.808	102			2.4284	130	5.4	1.8336	1.8371	1-14			1.4639	03-4
19.2	3.718	3.717	10-1			2.4301	21-1	11.7	1.7807	1.7795	040			1.4624	10-4
0.8	3.630	3.646	11-1	3.5	2.4185	2.4130	1-13	9.1	1.7723	1.7740	12-3	10.2	1.3763	1.3785	415
32.9	3.568	3.559	020	11.6	2.3747	2.3726	030	5.8	1.7647	1.7658	14-1			1.3743	405
24.6	3.483	3.475	120			2.3676	-201			1.7646	2-31			1.3722	05-2
100.0	3.392	3.397	112	17.8	2.3666	2.3567	213	14.1	1.7437	1.7432	412			1.3732	42-1
		3.394	201	20.1	2.3273	2.3199	022			1.7415	3-22	1.9	1.3621	1.3679	523
10.8	3.323	3.318	02-1	21.4	2.2600	2.2592	003	19.6	1.7052	1.7074	3-21	26.1	1.3569	1.3609	051
		3.305	121	69.4	2.2300	2.2315	01-3			1.7075	2-1-2	6.7	1.2427	1.2412	515
82.0	3.210	3.212	01-2	11.7	2.2153	2.2165	2-21	55.7	1.6952	1.6983	224	0.7	1.2386	1.2377	510
12.0	3.032	3.029	1-1-1	24.4	2.1980	2.1942	231			1.6944	004			1.2381	520
1.6	3.007	3.007	021	6.0	2.0994	2.1074	1-31	11.3	1.6586	1.6597	2-24	4.0	1.2172	1.2165	41-2
39.2	2.934	2.927	012			2.1026	322	0.3	1.6548	1.6524	242	9.0	1.2148	1.2136	416
11.0	2.894	2.893	1-21			2.0992	2-1-1	8.7	1.6521	1.6531	23-2				

Conditions: Goniometer HZG4 with 250 mm measuring circle radius, step-scanning in range 10 - 80° 2θ with step width 0.02° 2θ and 17 sec. exposition per step, PSF = Pearson VII.
Lattice parameters from powder data: $a = 6.973(3)$, $b = 7.361(7)$, $c = 7.662(5)$ Å, $\alpha = 90.024(9)$, $\beta = 62.999(9)$, $\gamma = 76.880(9)°$

References

ARNOLD, H. (1983): Transformations in crystallography. *In* International Tables for X-ray Crystallography, Volume **A** (T. Hahn, ed.). Reidel, Dordrecht, The Netherlands (69-75).

_____ (1989): Transformations in crystallography. *In* International Tables for X-ray Crystallography, Brief Teaching Edition of Volume **A** (T. Hahn, ed.). Kluwer, Dordrecht, The Netherlands (47-53).

BERMAN, H. & GONYER, F.A. (1937): The structural lattice and classification of bustamite. *Am. Mineral.* **22**, 215-216.

BRESE, N. E. & O'KEEFFE, M. (1991): Bond-valence parameters for solids. *Acta Crystallogr.* **B47**, 192-197.

DOWTY, E. (1991): *ATOMS, a Computer Program for Displaying Sructures.* Shape Software, Kingsport, Tennessee.

ĎUROVIČ, S. (1992): Layer stacking in general polytypic structures. *In* International Tables for X-Ray Crystallography **C**. Kluwer Academic Publisher, Dordrecht, The Netherlands (667-680).

HENMI, C., KAWAHARA, A., HENMI, K., KUSACHI, I. & TAKÉUCHI, Y. (1983): The *3T*, *4T* and *5T* polytypes of wollastonite from Kushiro, Hiroshima Prefecture, Japan. *Am. Mineral.* **68**, 156-163.

_____, KUSACHI, I., KAWAHARA, A. & HENMI, K. (1978): *7T* wollastonite from Fuka, Okayama Prefecture. *Mineral. J. (Japan)* **9**, 169-181.

HESSE, K.-F. (1984): Refinement of the crystal structure of wollastonite-*2M* (parawollastonite). *Z. Kristallogr.* **168**, 93-98.

_____, NARITA, H. & LIEBAU, F. (1982): Parabustamit $(Ca,Mn)_3[Si_3O_9]$-*2M*: Synthese und Kristalstruktur. *Z. Kristallogr.* **159**, 58-59.

INTERNATIONAL TABLES FOR X-RAY CRYSTALLOGRAPHY, Vol. IV (1974): The Kynoch Press, Birmingham, England.

LIEBAU, F. (1985): *Structural Chemistry of Silicates.* Springer-Verlag, Berlin, Germany.

OHASHI, Y. (1984): Polysynthetically-twinned structures of enstatite and wollastonite. *Phys. Chem. Minerals* **10**, 217-229.

_____ & FINGER, L.W. (1976): Stepwise cation ordering in bustamite and disordering in wollastonite. *Annual Report of the Director of Geophysical Laboratory, Carnegie Inst. Washington, Year Book* **1976-1977**, 746-752.

_____ & _____ (1978): The role of octahedral cations in pyroxenoid crystal chemistry. I. Bustamite, wollastonite and the pectolite – schizolite – serandite series. *Am. Mineral.* **63**, 274-288.

ONDRUŠ, P. (1995): ZDS system, version 6.01 – a computer program for analysis of powder X-ray diffraction data. ZDS system, Prague, Czech Republic.

PAUTOV, L.A., BELAKOVSKII, D.I., SKÁLA, R., SOKOLOVA, E.V., IGNATENKO, K.I. & MOKHOV, A.V. (1992): Vistepite $Mn_5SnB_2Si_5O_{20}$ – a new borosilicate of manganese and

tin. *Zap. Vses. Mineral. Obshchest.* **121**(4), 107-112 (in Russ.).

PEACOR, D.R. & BUERGER, M.J. (1962): Determination and refinement of the crystal structure of bustamite, $CaMnSi_2O_6$. *Z. Kristallogr.* **117**, 331-343.

_____ & PREWITT, C.T. (1963): Comparison of the crystal structures of bustamite and wollastonite. *Am. Mineral.* **48**, 588-596.

PETŘÍČEK, V. (1994): Computing system SDS 94, user's guide. Version April 1994. Edited by Ctirad Novák, Institute of Physics, Academy of Sciences of the Czech Republic.

_____ & MALÝ, K. (1990): SDS. A system of computer programs for the solution of structures from X-ray diffraction data. Unpubl. Rep., Institute of Physics, Academy of Sciences of the Czech Republic.

PICHOIR, F. & POUCHOU, J.L. (1991): SAMx STRATA Manual, software version 1.2 (1st ed., publ. **9101-F**). SAMx, Guayancourt, France.

PREWITT, C.T. & BUERGER, M.J. (1963): Comparison of the crystal structures of wollastonite and pectolite. *Mineral. Soc. Am., Spec. Pap.* **1**, 293-302.

_____ & PEACOR, D.R. (1964): Crystal chemistry of the pyroxenes and pyroxenoids. *Am. Mineral.* **49**, 1527-1542.

RAPOPORT, P.A. & BURNHAM, C.W. (1973): Ferrobustamite: the crystal structures of two Ca, Fe bustamite-type pyroxenoids. *Z. Kristallogr.* **138**, 419-438.

TEMPLETON, D.H. & TEMPLETON, L.K. (1978): Program AGNOST C. Univ. of California at Berkeley, Berkeley, California.

TROJER, F.J. (1968): The crystal structure of parawollastonite. *Z. Kristallogr.* **127**, 291-308.

YAMANAKA, T., SADANAGA, R. & TAKÉUCHI, Y. (1977): Structural variation in the ferrobustamite solid solution. *Am. Mineral.* **62**, 1216-1224.

YVON, K., JEITSCHKO, W. & PARTHÉ, E. (1977): LAZY PULVERIX, a computer program for calculating theoretical X-ray and neutron diffraction powder patterns. *J. Appl. Crystallogr.* **10**, 73-74.

Received May 2, 1996, revised manuscript accepted August 21, 1997.